https://doi.org/10.5194/essd-2023-359
Preprint. Discussion started: 24 October 2023

Open Access Earth System Science Data Discussions

Lagrangian surface drifter observations in the North Sea: An overview on high resolution tidal dynamics and submesoscale surface currents

Lisa Deyle[1], Thomas H. Badewien[1], Oliver Wurl[1], Jens Meyerjürgens[1]

[1]Center for Marine Sensors, Institute for Chemistry and Biology of the Marine Environment, University of Oldenburg, Oldenburg, 26129, Germany

Correspondence to: Lisa Deyle (lisa.deyle1@uni-oldenburg.de)

Abstract. A dataset of 85 Lagrangian surface drifter trajectories covering the central North Sea area and the Skagerrak from 2017 – 2021 of 17 deployments is presented. The data have been quality controlled, uniformly structured and assimilated in a standard NetCDF format. Using appropriate methods presented in detail here, surface currents were calculated from the drifter position data and gridded surface current maps with 0.125° spatial resolution were derived. The maps present for the first time mean currents of the south-eastern North Sea and the Skagerrak from Lagrangian observations. Tidal energy spectra were analyzed separately for the southern and northern areas of the North Sea, and tidal ellipses were calculated to determine the tidal impact on surface currents. Significant differences between the shallow shelf and the deeper areas of the North Sea are evident. While the shallow nearshore areas are dominated by tidal currents, deeper areas such as the Skagerrak register a high mean residual circulation driven by high density gradients.

Measurements using Eulerian approaches and remote sensing methods are restricted in temporal and spatial coverage, in particular, to capture submesoscale dynamics. For this reason, Lagrangian measurements, to a large extent, provide new insights in the complex submesoscale dynamics of the North Sea. Exemplarily, the Skagerrak region is used to illustrate the ability of reconstructing mesoscale and submesoscale current patterns using drifter observations.

This unique dataset covering the entire south-eastern North Sea and the Skagerrak offers further analysis possibilities and can be used for the investigation of various hydrodynamic and environmental issues, e.g., the analysis of submesoscale current dynamics at ocean fronts, the determination of the kinetic eddy energy and the propagation of pollutants in the North Sea.

https://doi.org/10.5194/essd-2023-359
Preprint. Discussion started: 24 October 2023

1 Introduction

The North Sea is one of the most intensely used coastal areas worldwide, connecting the major ports of Europe with the world oceans. The region is of particular interest to various stakeholders due to the economic and industrial value of its numerous riparian states. Industrial coastal activities, busy shipping lanes and growing offshore activities in the context of power generation with offshore wind farms increase the anthropogenic pressure on the marine ecosystem.

The North Sea is a semi-enclosed shelf sea opening in the north into the Norwegian Sea and in the western part into the English Channel. It is highly influenced by freshwater runoffs of the rivers Elbe, Scheldt, Rhine and Weser. Due to its shallow water depth in the majority of the area, it is highly impacted by strong tidal dynamics (Otto et al., 1990). Tides influence turbulence intensities and the energy cascades in shallow areas, which can create strong vertical mixing, enhancing the formation of tidal mixing fronts in the entire water column (Otto et al., 1990; Ricker et al., 2021). Furthermore it was shown that tidal motions have a scale-dependent influence on the relative diffusivities in tidal controlled shelf environments (Meyerjürgens et al., 2020). However, the particle motions are controlled by both the tides and the residual currents, the latter are mainly caused by density gradients.

Numerical models depend on in situ measurements to be developed further and for calibration purposes (Ricker et al., 2021; Ricker and Stanev, 2020). From 1970 to 1990, many investigations on tidal dynamics and surface currents, and thus the transport in the North Sea, have been reported in the literature (Becker et al., 1999; Otto et al., 1990). A dense network of monitoring stations was established in the last decades in the North Sea region, which makes it one of the best-observed coastal areas worldwide (Baschek et al., 2017). Nevertheless, further investigations are valuable because today's technical progress offers a higher quantity and quality of data and, in terms of spatial distribution, there still exist significant data gaps in the North Sea (Sündermann and Pohlmann, 2011). Previous studies of surface currents and tidal dynamics in the North Sea have consisted in deploying moorings with current meters that have taken long-term measurements using Eulerian measurement techniques (Davies and Furnes, 1980; Maas and van Haren, 1987). Other applications cover Acoustic Doppler Velocity Profilers (ADCP) mounted on ferries to gather current data on ferry routes (Vindenes et al., 2018). Similarly, near-shore high-frequency radars or satellite altimeters have been used to study surface currents (Baschek et al., 2017). One major drawback of all these measurement techniques is their focus on fixed points of regions covering distinct timescales, or in the case of satellite altimeters, measurements are continuous in space and time, but with coarse resolution.

In contrast, Lagrangian measurement techniques, which have been rarely used in the North Sea (Meyerjürgens et al., 2019), are variable in space and time. They can capture small spatially and temporally rapid movements, as well as large-scale temporal variations (Lilly and Pérez-Brunius, 2021a). Lagrangian measurements can cover mesoscale ocean circulations, small-scale and submesoscale fluid dynamics to improve the understanding of complex surface current and energy dynamics (Lumpkin et al., 2017; Özgökmen et al., 2012). The processes at submesoscales (0.1 – 10 km length scale) can be observed at fine spatial and temporal resolution with Lagrangian techniques (McWilliams, 2016). Differential kinematic properties and dispersion characteristics of the submesoscale current field can be determined, allowing an understanding of the structure and

https://doi.org/10.5194/essd-2023-359
Preprint. Discussion started: 24 October 2023

dynamics of the ocean surface, for example, at density fronts (Essink et al., 2020; Tarry et al., 2022). Furthermore, several studies analyzed the propagation of particles and Lagrangian surface drifters at the sea surface to understand the ecological implications of plastic litter (Van Sebille et al., 2020; Meyerjürgens et al., 2023) and oil spills (Liu and Weisberg, 2011) in open ocean and coastal areas. For this reason, a satellite-tracked high-resolution surface drifter, which is adjustable with various wind slip characteristics, was developed that follows surface currents at 0.5 m depth and can be used in tidally influenced coastal and estuarine areas (Meyerjürgens et al., 2019) as well as in open ocean environments (Martín et al., 2023).

This study presents drifter data collected from 2017 to 2021 in the North Sea. Previously, only individual datasets have been analyzed for individual scientific objectives. This paper provides an overview of the coverage of all collected data, resulting in a comprehensive Lagrangian dataset that contributes to a better understanding of the circulation and tidal dynamics in the North Sea. The large number of Lagrangian observations based on drifter studies provide data covering large temporal and spatial scales and is presented for the North Sea for the first time due to a significant lack of studies using drifters in the past. Thus, this study presents a comprehensive dataset and investigates the tidal dynamics and provides furthermore a Lagrangian observational view for the first time for the North Sea. The particular focus will be on presenting the dataset and describing the processing methods in detail. In addition, the calculated current velocities will be compared with other data to prove the reliability of the methods.

2 Study Area

The North Sea is a semi-enclosed shelf sea surrounded by Great Britain and central northern continental Europe. At the northern edge, it is connected to the Norwegian Sea and the North Atlantic by a broad opening, whereas in the south, it is narrowly linked by the English Channel to the North Atlantic (Fig. 1). In addition, to the high saline Atlantic water, the North Sea gains a substantial inflow of the low saline Baltic water and freshwater inflows from river runoffs (Otto et al., 1990).

The average depth of the North Sea is around 80 m, becoming shallower from north to south toward the coast (Otto et al., 1990; Vindenes et al., 2018). The Norwegian Trench and the Skagerrak as an extension are the deepest region with a sill depth of approximately 270 m and a maximum depth of 700 m (Vindenes et al., 2018).

The tides in the North Sea are initiated by tidal waves from the North Atlantic. This emerges from the Norwegian Sea, moves along the coast of Great Britain and propagates around three amphidromous points in the North Sea. These are located at the south-western tip of Norway, at the eastern tip of Dogger Bank and near the entrance to the Southern Bight. The dominant tidal component is the tidal motion of the semidiurnal M_2 tide and provides a good initial approximation of the tidal motion. Tidal currents can reach maximum velocities above 1 m s^{-1} for spring tides in the shallow southern part of the North Sea and along the coast of Great Britain (Dietrich, 1950; Valle-Levinson et al., 2018). In the deeper northern part, maximum velocities of some tens of cm s^{-1} are reached (Otto et al., 1990), and lowest in the Skagerrak with a magnitude of 1 cm s^{-1} (Danielssen, 1997; Rodhe, 1987).

https://doi.org/10.5194/essd-2023-359
Preprint. Discussion started: 24 October 2023

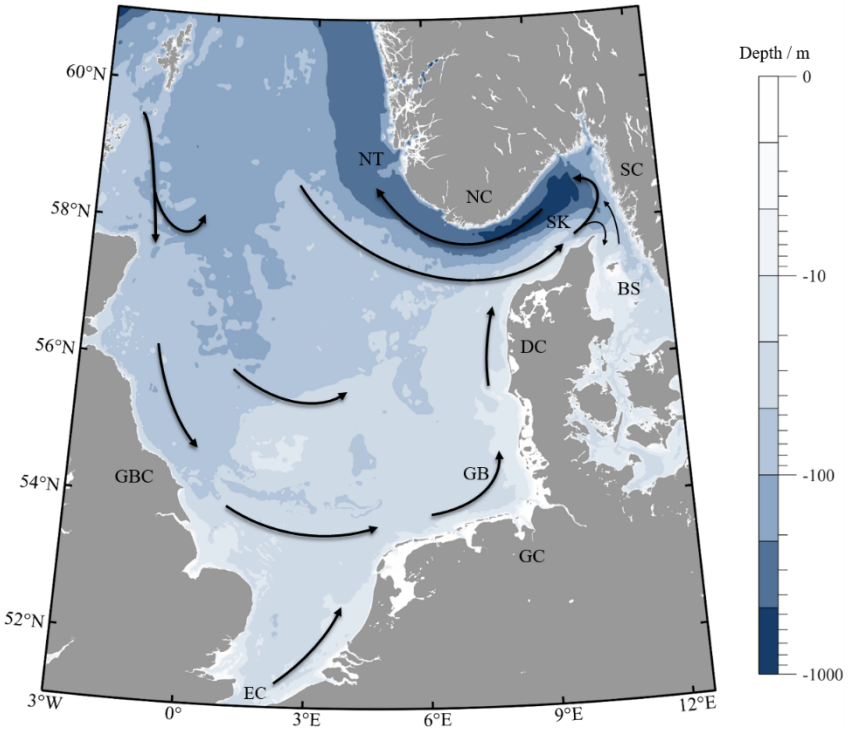

Figure 1: A map of the North Sea and its surroundings, showing the major mean ocean circulation pattern in the North Sea. Acronyms: Baltic Sea (BS), Danish Coast (DC), German Bight (GB), Great Britain Coast (GBC), German Coast (GC), Norwegian Coast (NC), Norwegian Trench (NT), Swedish Coast (SC), Skagerrak (SK) (based on Otto et al. (1990)).

In addition to the cyclic tidal components such as M_2, averaging the tidal currents result in residual currents. These are partly due to nonlinear tidal interactions. In the shallow coastal regions of the North Sea, nonlinear tidal interactions can occur due to shallow water tides that deform the original sinusoidal character of the tide (Otto et al., 1990). Overtides are generated due to advection terms, such as the M_4 tide, which occurs twice as often as the semidiurnal M_2 tide, and odd harmonics (e.g., M_6) are generated due to bottom friction (Le Provost, 1991; Stanev et al., 2016). They can be essential for tidal dynamics in shallow water areas. Other residual currents are due to prevailing westerly winds and varying density gradients due to freshwater inputs, mainly from the Rhine, Ems, Weser, and Elbe rivers (Otto et al., 1990; Ricker et al., 2020).

The residual currents lead to a permanent displacement of water masses, forming a cyclonic residual circulation (Otto et al., 1990; Burchard and Badewien, 2015). Thus, the circulation turns eastward at the southern part of the coast of Great Britain, flows further along the coast of Germany, and then flows northward along the Danish coast into the Skagerrak (Fig. 1). It should be noted that strong, persistent winds from the south and east can weaken or even reverse the circulation pattern (Howarth, 2001). In the shallow area of the North Sea, the residual circulations are assumed to be smaller compared to tidal currents and wind-induced currents. In contrast, in deeper areas, such as the Skagerrak, the surface currents are driven by strong density differences resulting from strong inflows from the North Atlantic, North Sea, Baltic Sea, and river runoffs, so the residual circulations are more extensive in this area (Howarth, 2001).

https://doi.org/10.5194/essd-2023-359
Preprint. Discussion started: 24 October 2023

3 Material and Methods

The dataset presented here was obtained using GPS (Global Positioning System) data from satellite-tracked surface drifters, which state-of-the-art design is compact, cost-effective, and light-weight (Fig. 2). The drifters are designed to follow the upper 0.5 m surface currents by four cruciform drag-producing vanes to minimize the direct wind slip effect. The drag area ratio which is a measure for the direct wind slip were calculated by Meyerjürgens et al. (2019) accounting for 0.27 % resulting in wind-induced velocities ranging from 0.0027 – 0.027 m s^{-1} by wind speed amplitudes of 1 – 10 m s^{-1}.

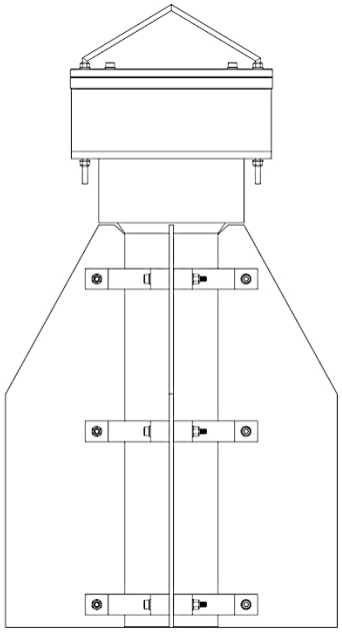

Figure 2: A drawing of the Lagrangian satellite-tracked high resolution surface drifter.

In contrast to many other drifters, this one can be deployed in shallow water environments and can be resuspended in coastal areas after it has washed ashore. A detailed description of the drifter can be found in Meyerjürgens et al. (2019).

This section describes the data processing and quality control, and further presents the methods to analyze the tidal dynamics and the surface current fields. First, the various deployments of the drifters are presented (Sect. 3.1). In Sect. 3.2, the drifter data processing including quality control, outlier removal and interpolation schemes are presented. In the next section, the method used to calculate the drifter velocities and the residual currents is explained (Sect. 3.3). Finally, in Sect. 3.4 the analysis of the tidal dynamics including the calculation of the power spectral density is given.

3.1 Drifter Deployments

The drifters were deployed on different ship expeditions from 2017 to 2021 and measured in some cases for several months (Tab. 1).

https://doi.org/10.5194/essd-2023-359
Preprint. Discussion started: 24 October 2023

Open Access Earth System Science Data Discussions

Table 1: Information for the surface drifter datasets in the North Sea. From left to right: name of experiment; deployment area; original sample interval in minutes; number of trajectories; number of 5-minute data points after interpolation; percentage how often drifters did not transmit over an hour; date of first data point within a deployment; date of last data point within a deployment; mean duration of a deployment in days; plus or minus the standard deviation of trajectory durations in days; maximum trajectory duration in days. Datasets were sorted by year (based on Lilly and Pérez-Brunius (2021a)).

Surface drifter data from the North Sea									
Name	Area	Interval / min	Traj.	Points	Fill / %	First Date	Last Date	Duration / d	Max / d
Mar17	German Bight	10	6	39188	0.304	13-Mar-2017	22-Apr-2017	23±14	40
Aug17	German Bight	10	2	7501	0.536	02-Aug-2017	24-Aug-2017	13±13	22
Oct17	German Bight/Southern Denmark	10	5	17391	0.282	08-Oct-2017	27-Oct-2017	12±4	15
Feb18	North Sea	10	6	164636	0.239	24-Feb-2018	25-Jun-2018	95±19	116
Oct18	German Bight/Denmark/Norway	10	15	265168	1.373	21-Oct-2018	22-Jan-2019	61±22	93
Mar19	Southern German Bight	10	7	8896	0.483	22-Mar-2019	27-Mar-2019	4±0	5
Jul19	German Bight/Denmark	10	11	94993	0.638	12-Jul-2019	12-Aug-2019	30±1	31
Jul21	German Bight	5	6	48636	0.157	22-Jul-2021	25-Aug-2021	28±4	35
Sep21	(Eastern) German Bight	5	10	45066	0.122	12-Sep-2021	05-Oct-2021	16±6	23
Oct21	Skagerrak	5	17	117635	0.214	07-Oct-2021	24-Nov-2021	24±14	48
ALL	North Sea	5	85	809110	0.435	13-Mar-2017	24-Nov-2021	31±10	116

They are equipped with a GPS tracker that transmits the coordinates of the drifter position and time by satellite. Depending on the measurement strategy a transmission interval of 5 or 10 minutes was set. As a result, 85 high-resolution trajectories could be measured during the entire period, which are shown in Fig. 3. In 2017, the drifters were deployed in clusters in different areas of the German Bight (Fig. 3a). Similarly, in 2018, all drifters were deployed in the German Bight, but the measurements captured a larger area because the drifters covered a period of at least 39 days (Fig. 3b). Many drifters were transported northward into the Skagerrak with the typical circulation trend of the North Sea, but due to a strong sustained easterly wind in early 2018, some drifters moved eastward (Ricker et al., 2020; Stanev et al., 2019). A short drifter deployment in the southern German Bight was realized in spring 2019, as well as a longer measurement of about 30 days along the German-Danish coast in summer (Fig. 3c). After a break in measurement in 2020, three larger measurement campaigns followed in 2021, two in the German Bight, the third for the first time in the Skagerrak, where 17 drifters were deployed along a transect (Fig. 3d).

https://doi.org/10.5194/essd-2023-359
Preprint. Discussion started: 24 October 2023

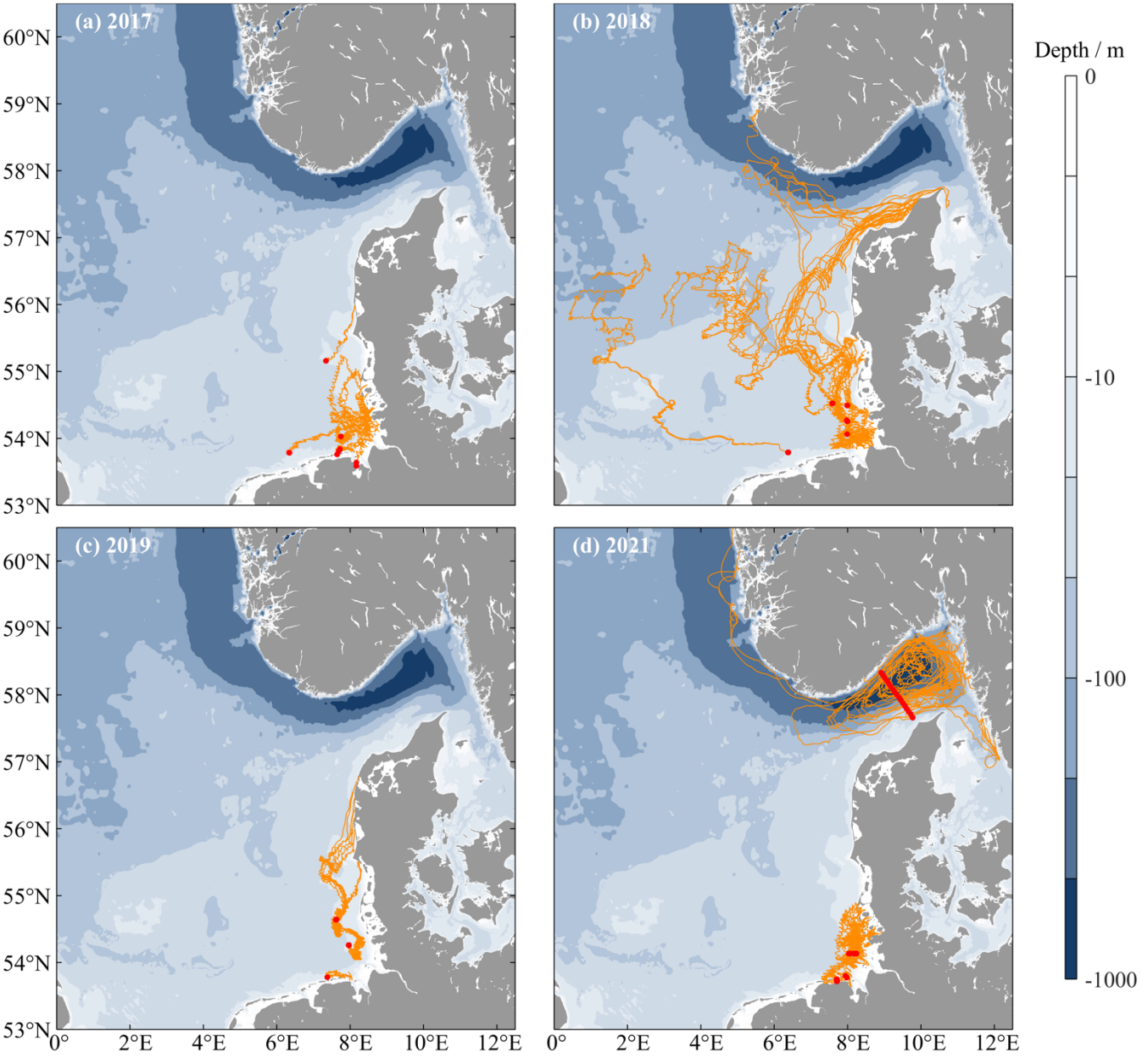

Figure 3: Processed and interpolated surface drifter data in the North Sea from 2017 (a), 2018 (b), 2019 (c) and 2021 (d). The starting points of the trajectories are indicated by red dots.

3.2 Data Processing

In order to use the data, several processing steps had to be taken. First, the raw data were cut so that beachings were removed. In the next step, outliers were eliminated from the latitude and longitude data with a hampel median filter. The filter calculates

https://doi.org/10.5194/essd-2023-359
Preprint. Discussion started: 24 October 2023

the median and standard deviation for each sample value for a window of 18 surrounded samples (9 per side). All drifter positions that deviate from the median by more than three standard deviations are replaced by the median in the time series dataset. In the present study, 0.041 % of the total dataset deviates from the median by more than three standard deviations, indicating that the dataset has only a small number of outliers that had to be replaced. As drifter positions were measured at irregular time intervals, in a final step all data was interpolated using a piecewise cubic interpolation method (Fritsch and Carlson, 1980), also known as the pchip method. For an overview, the individual interpolated data points, with the 5-minute intervals, were summed to show the total number of data collected by the drifter after the interpolation (Tab. 1). The percent of filled data describes how often data gaps of more than one hour occurred. These data gaps are caused by data transmission errors, which can occur especially in bad weather conditions. During strong winds and high waves, the drifters are washed over more frequently, which can restrict the communication between the satellites and the GPS trackers of the drifters. The interpolated data is considered 'filled' if no data has been supplied in the raw dataset for more than one hour. This affects, as seen in Tab. 1, an average of only 0.435 % of the collected data. This proves their reliability and the high quantity and high-resolution of data sent by the drifters.

Finally, all data were sorted by assimilating into a standard NetCDF format. The dataset contains drifter position data (*lat*, *lon*, *datenum*, *time*), drifter derived current velocities (*u*, *v*) and two vectors (*beached*, *filled*) describing when a drifter was beached and when the dataset was filled because no GPS position was sent for more than one hour. All data are associated with a drifter ID (*drifter_id*) and a deployment ID (*deploy_id*) to identify which data belongs to a drifter and when multiple drifters have been deployed in a single deployment.

3.3 Velocity Calculation

The current velocities can be calculated with a forward difference scheme (Eq. 1, 2):

$$u_d = \frac{x_d(t+\delta t) - x_d(t)}{\delta t} \quad (1)$$

and

$$v_d = \frac{y_d(t+\delta t) - y_d(t)}{\delta t} \quad (2)$$

where $x_d(t)$ and $y_d(t)$ are the zonal and meridional coordinates, δt is the time interval and u_d and v_d are the zonal and meridional velocity components.

The first step involves the extraction of the position data for a selected region. This can be done by setting limits for the latitude and longitude values or by selecting the desired expeditions or deployments from the NetCDF structure. In the next step, the longitude and latitude coordinates in degrees must be converted to zonal and meridional coordinates $(x_d(t), y_t(t))$. Afterwards, the forward difference method is used to calculate the zonal u_d and meridional v_d velocity components from the zonal and meridional coordinates determined at time t (Eq. 1, 2). The complex-valued velocity $cv = u_d + \sqrt{-1} \cdot v_d$ in m s^{-1} is determined from the zonal and meridional velocity components u_d and v_d.

https://doi.org/10.5194/essd-2023-359
Preprint. Discussion started: 24 October 2023

It is important to note that the velocity components u_d and v_d include both, the tidal and the residual currents. To represent the mean residual circulations, the tidal component must be extracted. Therefore, a moving average filter is used over a 24.83 - hour period, which low-pass filters the velocity time series. With this time period the dominant tidal constituents for the North Sea, such as M_2 and S_2, are removed. The moving average filter removes these tidal constituents from the zonal and meridional current velocities u_d and v_d.

In order to get an overview of the mean surface velocities in an area, a grid is created that is composed of several cells. The individual velocities are assigned to the corresponding cell and an average value is calculated for each cell; data gaps are represented as NaN (Not a Number). For the data in this study, a latitude range of 54° N to 60.5° N was chosen and a longitude range of 4° E to 12.5° E with a cell resolution of 0.125° in both directions.

Furthermore, the velocity calculation can be used to consider both mesoscale and submesoscale dynamics. Within the grid, the latitude and longitude cell resolution must be adjusted accordingly for the velocity calculation. For the Skagerrak data, cell resolutions of 15 km, 7.5 km, 5 km, and 3 km were chosen, revealing the differences between submesoscale and mesoscale processes. Cells where no drifter data are available are replaced by approximated values. The 5 cells in horizontal and vertical direction surrounding the data gap are used for the approximation. With these values from the 5-by-5 moving window, a mean value is calculated, which replaces the data gaps.

3.4 Tidal Analysis

3.4.1 Power Spectral Density

The raw velocity time series signal of u_d and v_d are used to observe the tidal effects. Due to their periodic behaviour, the tidal currents can be decomposed into their harmonic fundamental components with their representative frequency. If a time series is of appropriate length, the tidal constituents at any location can be determined. The main tidal constituents of the North Sea that have been considered in more detail in other studies are listed in Tab. 2 (Meyerjürgens et al., 2019; Otto et al., 1990; Vindenes et al., 2018). For the representation of tidal currents in the frequency domain, the power spectral density (PSD) is suitable. The power spectral density is used when non-periodic components are present in the signal in addition to periodic components. These signal types are called as random signals. This is useful for the signals in this study, since non-linear influences, such as different wind strengths, can also affect the signal. As in a standard Fourier transform, the signal is decomposed into the individual frequencies, but at the same time the power spectral density describes the proportion of different frequencies over the total power and indicates the energy distribution of a signal (Dempster, 2001). The power spectral density is normalized to a single hertz bandwidth, giving a uniform value regardless of the bandwidth.

The first step is to select the region where the tidal currents are to be analyzed. In this study, the latitude ranges < 55° N, 55° N - 57° N and > 57° N were chosen. Already Otto et al. (1990) divided the North Sea in their study into a southern, a central and a northern section, in which different dynamics are to be expected. The velocity time series are assigned to these regions. Trajectories that are located in multiple regions are divided into individual time series data and assigned to the appropriate

https://doi.org/10.5194/essd-2023-359
Preprint. Discussion started: 24 October 2023

region. In addition, a minimum signal length should be established. The velocity time series should be of a sufficient length to filter tidal constituents as accurately as possible and short enough that a large number of time series can be included in an analysis to provide a suitable power spectral density. Since a power spectral density is always decomposed into a respective power of two of the signal length, in this analysis a time series with a minimum of 4096 intervals ($2^{12} = 4096$) was chosen, which corresponds to a period of about 14.2 days. For each velocity time series of the corresponding length, the power spectral density is determined. In the last step, the individual power spectral densities from the same region are averaged so that a mean power spectral density can be presented for each region (< 55° N, 55° N - 57° N and > 57° N).

Table 2: Main tidal constituents of the tides in the North Sea. Period is given in hours, frequency in cycles per day.

Description	Symbol	Period / h	Frequency / d^{-1}
Principal lunar semidiurnal constituent	M_2	12.4206	1.9323
Principal solar semidiurnal constituent	S_2	12.0000	2.0000
Shallow water overtides of principal lunar constituent	M_4	6.2103	3.8645
Shallow water overtides of principal lunar constituent	M_6	4.1402	5.7968
Shallow water overtides of principal lunar constituent	M_8	3.1052	7.7291
Luni-solar diurnal constituent	K_1	23.9345	1.0027
Lunar diurnal constituent	O_1	25.8193	0.9295

3.4.2 Tidal Ellipses

Similar to the calculation of the power spectral density, the unfiltered time series of complex-valued velocities *cv* are taken to calculate and display tidal ellipses. They are used to analyze the individual tidal constituents using the tidal harmonic analysis toolbox *t_tide* by Pawlowicz et al. (2002). It should be noted that only sufficiently long time series are taken. In this study, a length of at least 3000 intervals (10.4 days) was specified, since a Fourier transform yields plausible results above this length. The tidal extraction results can be plotted using the tidal ellipse parameters of a tidal constituent provided by *t_tide*. The tidal ellipse is characterized by the major axis constituent *fmaj*, the minor axis constituent *fmin*, and the ellipse orientation *finc*, which describes the inclination angle (Fig. 4). The major axis represents the maximum and the minor axis the minimum tidal current velocity of the respective tidal component. The ellipse orientation describes the angle between the eastward direction and the major axis counter clockwise. In the last step, all tidal ellipse parameters of the individual time series are averaged so that an averaged ellipse is determined for an area. This study focuses on the analysis of the lunar semidiurnal M_2 tide, as this tide is the most dominant tidal component of the North Sea. Other tidal components can be computed using the same procedure.

https://doi.org/10.5194/essd-2023-359
Preprint. Discussion started: 24 October 2023

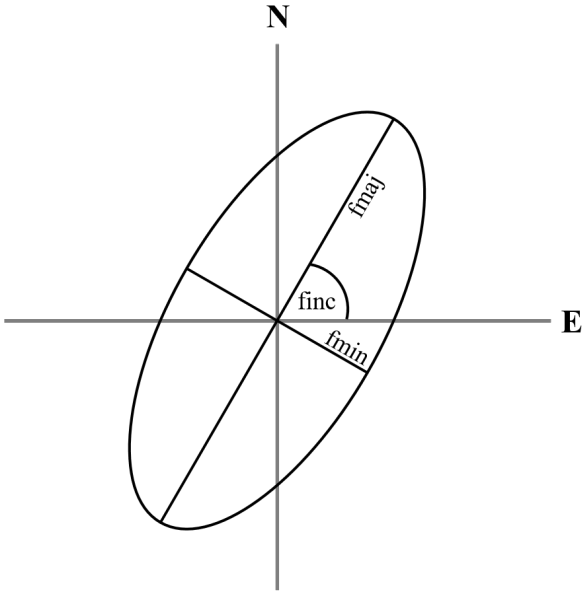

Figure 4: Illustration of a tidal ellipse. *fmaj* is the major axis, *fmin* the minor axis, they describe the maximum and minimum velocity of the tidal currents. *finc* is the inclination of the ellipse and describes the angle between the east direction and the major axis counter clockwise (based on Vindenes et al. (2018)).

4 Results

The trajectories in Fig. 3 reflect the circulation pattern in the North Sea. Southern drifters, for example from spring 2019 (Fig. 3c), are transported eastward along the northern German islands. The drifters in the eastern German Bight are transported along the Danish coast into the Skagerrak. In this area, the drifters spread with the eastern inflow from the North Atlantic, or along the northern slope in the opposite direction with the Norwegian Coastal Current. Individual drifters from 2018 were transported contrary to the typical circulation pattern to the west and not into the Skagerrak, due to a strong sustained easterly wind during this period (Ricker et al., 2020; Stanev et al., 2019) (Fig. 3b). These are extreme events in the North Sea and would bias the results. We have removed these extreme events for the analysis of the mean residual circulation of the surface currents, but in case of interest these data can be found in the supplements (Fig. S1). Using the method from Sect. 3.3, mean residual surface velocities can be determined for the North Sea based on the drifter data, which are shown in Fig. 5. The arrows indicate the directional components of the mean residual velocities of u and v, and the length describes the magnitude of the velocity. The difference between the shallow shelf and the deeper areas of the North Sea are apparent. The shallow areas indicate very low residual velocities of u and v, ranging from about 0.01 - 0.1 m s^{-1}. This is due to the high residence time of a drifter inside a cell, which results in counteracting residual velocities. Despite the low residual velocities, the circulation pattern from south to north can be recognized on the west coast of Germany and Denmark. Furthermore, based on the slight increase of the meridional velocity component, it can be shown that the mean residual velocity increases from south to north (Fig. 5b). In the deeper part of the North Sea, as in the Skagerrak, much higher residual circulations are apparent (Fig. 5). The

https://doi.org/10.5194/essd-2023-359
Preprint. Discussion started: 24 October 2023

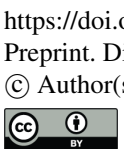

eastern inflow of the North Atlantic (orange-red) and the Norwegian Coastal Current (blue) are strongly visible with their velocities around 0.6 m s^{-1}. It should be noted that maximum values of up to 0.8 m s^{-1} were measured in a small number of cells. Changes in direction at the Norwegian-Swedish coast, as well as small eddies and the outflow into the Baltic Sea, are clearly visible. In addition to the described circulation pattern, small-scale directional changes of the drifter motions can be recognized, which can be for example further wind-driven currents or the convergence of drifters caused by ocean fronts.

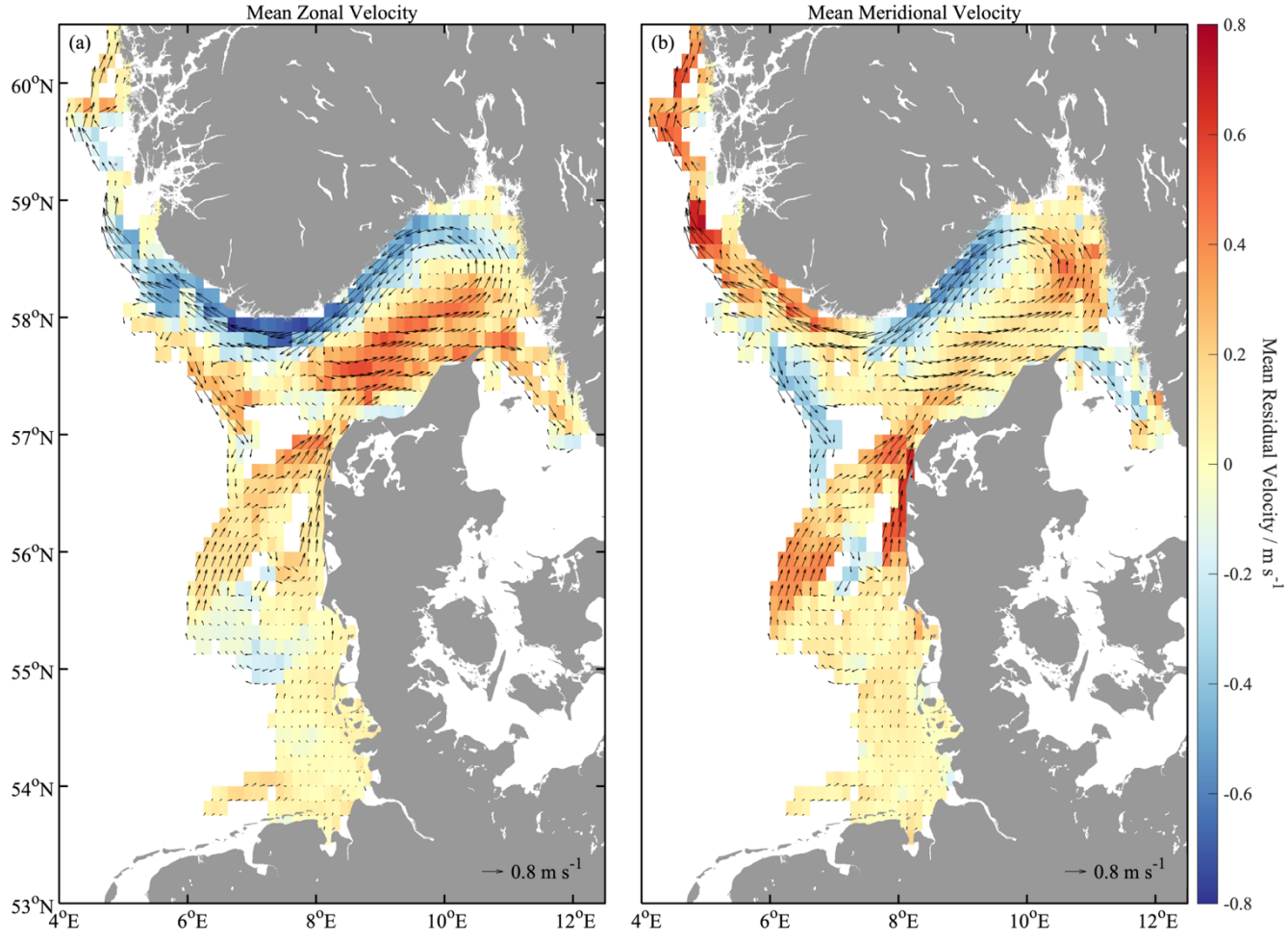

Figure 5: Mean velocities of the residual circulations for (a) the zonal component *u* and (b) the meridional component *v*. The arrows indicate the direction of the mean velocities, the magnitude describes the strength of the velocity.

The differences between the shallow shelf and the deeper regions can also be seen in the tidal ellipses of the semidiurnal M_2 tide (Fig. 6). For each blue ellipse, a latitude range of 2° was considered between 4° E - 9° E and for each red ellipse, a longitude range of 3° between 57° N - 60° N. The tidal dominance in the shallow water shelf is evident. It can be concluded that the shallower the North Sea and the greater the distance to the three amphidromous points, the higher the mean tidal

https://doi.org/10.5194/essd-2023-359
Preprint. Discussion started: 24 October 2023

currents become. Maximum mean current velocities are observed of up to 0.49 m s^{-1} in the southern German Bight and 0.12 m s^{-1} around the Danish coast. Furthermore, the elliptical orientation of the tide decreases from 145.4° to 123.6°, which means that the north-south motion increases. In the deep North Sea, the tidal wave has little effect on the circulation. In the Norwegian Trench only velocities of 1.3 – 6.5 cm s^{-1} are reached, in the Skagerrak velocities of 0.7 – 4.1 cm s^{-1}.

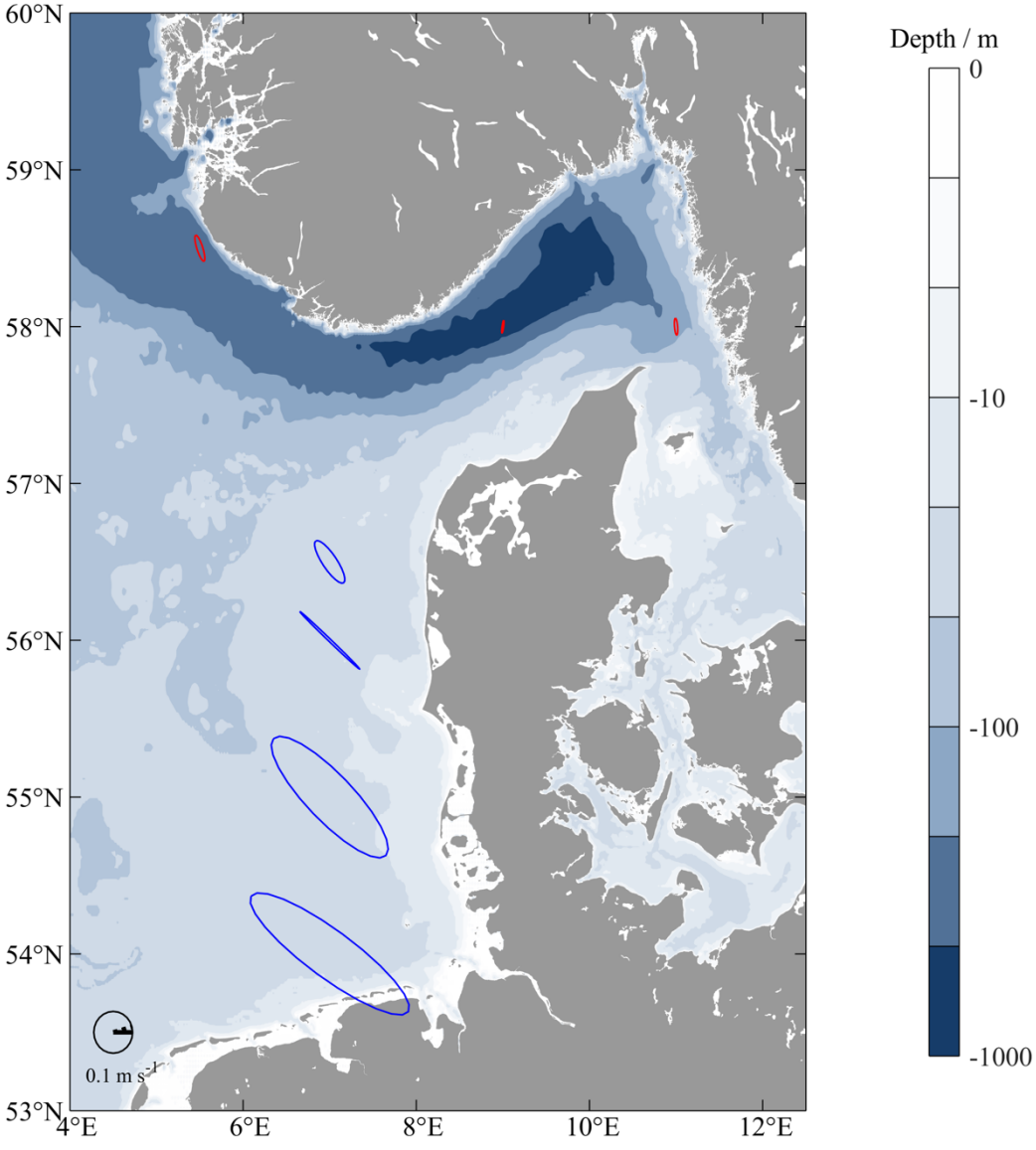

Figure 6: Calculated Mean tidal ellipses for the North Sea. The colours of ellipses describe the size of the cells used for the calculation: blue: 2° lat, 5° lon; red: 3° lat, 3° lon.

In addition, the analysis of the mean power spectral density provides further insights into the tidal analysis (see Sect. 3.4.1). The zonal component shows that in the southern region of the North Sea (< 55° N) the tides are most dominant (Fig. 7a). The

https://doi.org/10.5194/essd-2023-359
Preprint. Discussion started: 24 October 2023

peak of the dominant tidal constituent M_2 with 1.93 cycles per day is apparent. Furthermore, the shallow water tidal components M_4, M_6 and M_8 are shown with smaller peaks, as well as the solar semidiurnal tide constituent S_2. In latitude range of 55° N - 57° N, the peaks of the zonal M_2, M_4 and M_6 tides are also clearly visible, but the magnitude of M_6 is smaller. In the Skagerrak area, a weak elevation can be recognized in the area of the S_2 and M_2 tidal components. Other irregularities are difficult to distinguish from the rest of the noise. The mean power spectral densities of the meridional velocity time series show similar characteristics, but the peaks are not as dominant as those of the zonal mean power spectral densities and no peak is present in the frequency range of M_8 (Fig. 7b). Despite the fact that the overall meridional tidal motion is smaller, it increases towards the north (55° N - 57° N). In the deep area of the Skagerrak, the tidal currents are also not differentiable from the noise for the meridional components.

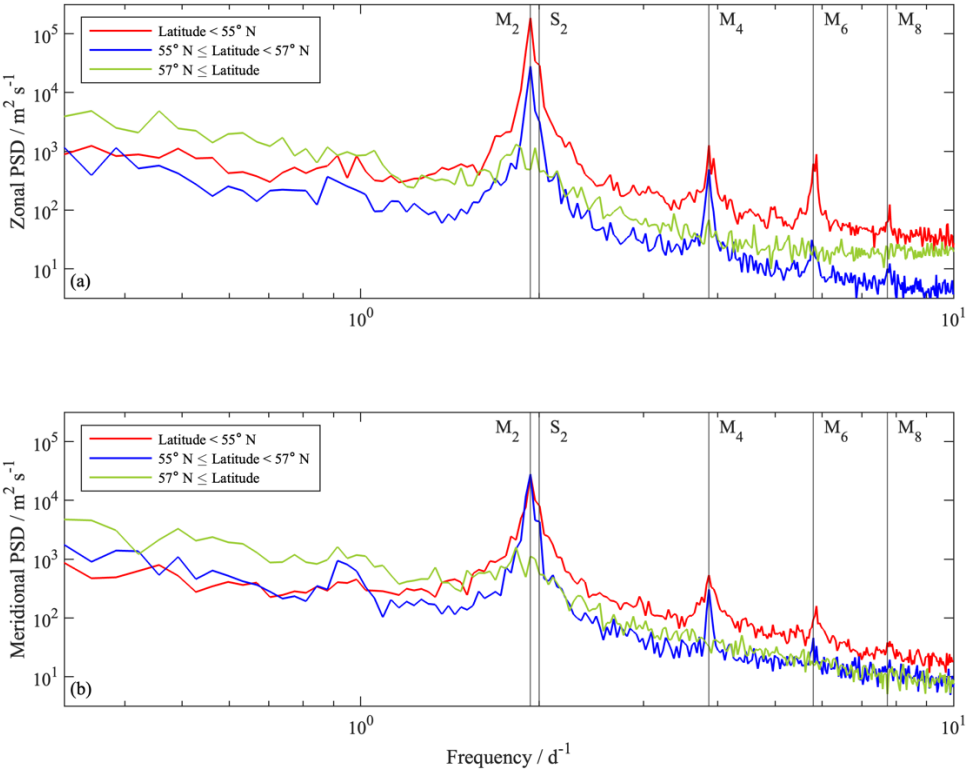

Figure 7: Mean power spectral density on (a) the zonal *u* and (b) the meridional *v* drifter velocities in the North Sea averaged over all trajectories. The periods of the semidiurnal and shallow water tidal components are indicated by the vertical lines.

The computation of the drifter velocity can also be used to highlight differences between mesoscale and submesoscale dynamics by adjusting the latitude and longitude resolutions (see Sect. 3.3, Fig. 8). With a cell resolution of 15 km, there are on average 358 drifter position data per cell available from which the velocity can be calculated. With 7.5 km cell resolution 90 values, with 5 km 40 values and with 3 km 17 values are available. The generally larger mesoscale current pattern due to

https://doi.org/10.5194/essd-2023-359
Preprint. Discussion started: 24 October 2023

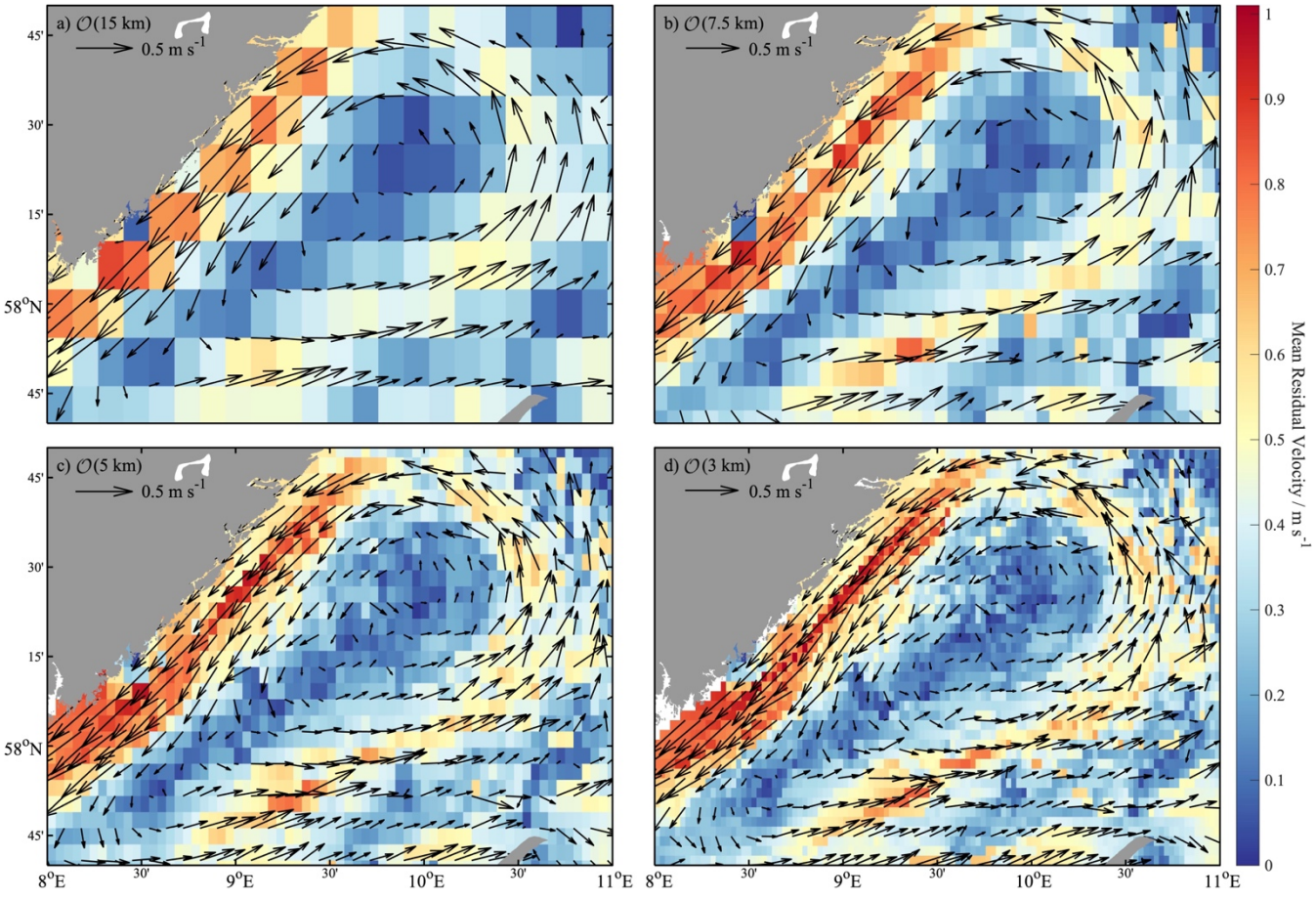

Figure 8: Mean velocities of the residual circulations in the Skagerrak with a) 15 km, b) 7.5 km, c) 5 km, and d) 3 km cell resolution. The arrows indicate the direction of the mean velocities, the magnitude describes the strength of the velocity.

5 Discussion

In this study, a comprehensive Lagrangian dataset is presented for the North Sea region for the first time. The dataset is valuable for various kinds of marine science research topics, e.g. marine litter transports and carbon or nutrient exchange processes, and provide important insights into the tidal dynamics, and complex surface current patterns in the region. Lagrangian surface drifters offer the ability to cover different areas with a single system because it moves with the current. The drifters provide the opportunity to gain an understanding of the transition processes between the mesoscale ocean circulation and the small-scale and submesoscale fluid dynamics (Lumpkin et al., 2017; Özgökmen et al., 2012). Large-scale and long-term fluctuations are captured, as well as small-scale and rapid motions (Lilly and Pérez-Brunius, 2021a). It is a simple and cost-effective system

https://doi.org/10.5194/essd-2023-359
Preprint. Discussion started: 24 October 2023

and is completely autonomous after being deployed (Meyerjürgens et al., 2019). In the past, the coverage of the entire North Sea in terms of current patterns has been only provided by satellite and remote sensing methods, but these techniques cannot provide the temporal and spatial resolution to understand the smaller-scaled and highly dynamic processes in the North Sea. Therefore, satellite and radar remote sensing observations are often combined with in situ platforms, resulting in the further development of model data for the North Sea (Baschek et al., 2017; Ricker and Stanev, 2020; Stanev and Ricker, 2020). For this reason, Lagrangian surface drifters provide platforms for area-wide in situ measurements and are essential to support and promote further development of model analysis and particle tracking approaches.

Computation of gridded-averaged surface current has been proven useful for a large-scale acquisition of current data. Lilly and Pérez-Brunius (2021a) have used a similar analysis and presentation methods for the Gulf of Mexico. Drifter derived circulation patterns showing surface currents advection from west to east at the southern German Bight and from south to north at the German-Danish coast are consistent with studies by Otto et al. (1990) and Huthnance (1991). The strong circulation pattern in the Skagerrak, which is driven by the mixing of saline Atlantic water (south slope) and fresh water from the Baltic Sea (north slope) (Rodhe, 1996), is strongly visible in the gridded representation. Model data from Ricker and Stanev (2020), which has been previously compared with high-frequency radar measurements and drift measurements, show that there is a transition between two regimes at the 200 m isobath that present strong differences in dynamics between the shallow and deep ocean. This study confirms that the shelf area as tidal dominated system is characterized by relatively low residual velocities of up to 0.1 m s^{-1}, which are consistent with the study results. The values from the model data in the Skagerrak of up to 0.5 m s^{-1} also show a similar magnitude (Ricker and Stanev, 2020). Although typical values of 0.6 m s^{-1} increasing occasionally up to 0.8 m s^{-1} are higher in this present study, but these values include a wind-driven flow component, so a higher value with a small deviation is realistic.

In addition, calculating the averaged surface currents with drifter position data allows the representation of submesoscale dynamics. Capturing submesoscale dynamics are challenging with ship-based measurements alone, due to the direct influence of the vessel on the surface layer and fine-scale structures. Remote sensing data often lacks in resolution and floats and gliders are not able to resolve the temporal scales at the submesoscales due to their measurements principles and, in addition, often exclude the ocean surface boundary layer (McWilliams, 2019). In this context, it is important to capture these dynamics because increasing evidence shows that accounting for the influence of submesoscales on oceanic energetics and tracer fluxes, can improve the fidelity of global ocean and climate models (Taylor and Thompson, 2023). Fig. 8 shows that high coverage of high-resolution drifter data can fill this gap of knowledge. Mesoscale as well as submesoscale processes can be analyzed simultaneously by adjusting the latitude and longitude cell resolution when calculating the averaged surface currents.

This study demonstrates the application of power spectral density to analyze tidal dynamics. The decomposition of velocity time series into their frequency domain is an established method. Meyerjürgens et al. (2020) used a Fourier transform to represent the frequency domain, which confirms the dominant M_2 tidal component for the North Sea, as well as the increased amplitudes for the frequencies of the shallow water components M_4 and M_6 and the solar semidiurnal S_2 component in the southern region of the North Sea. For comparison, a Fourier transform on the drifter dataset is also shown in the supplements

https://doi.org/10.5194/essd-2023-359
Preprint. Discussion started: 24 October 2023

(Fig. S2). In this study power spectral density was chosen, because of the additional insights to obtain the energy of a signal. Similarly, this approach supports the averaging of several time series as a frequency range of length of 2^x is generated and all frequency ranges are multiples of each other independent of the signal length.

The analysis of tidal ellipses has also been used for time series of current velocities. Vindenes et al. (2018) used tidal ellipses for an analysis of the northern North Sea using current data from ADCPs. It confirmed that the M_2 tide is the most dominant component and that similar magnitudes are obtained for the Skagerrak. The occurrence of the tidal ellipses of K_1 and O_1 cannot be confirmed based on the results of power spectral densities, since no peaks emerge from the power spectral densities. It should be noted that Vindenes et al. (2018) provides very small tidal amplitudes for K_1 and O_1, which may have been masked by the noise in the power spectral densities. Furthermore, the measurements were made at different depths. This present study considers tides at the surface, whereas Vindenes et al. (2018) measured at a depth of 53 m, which may led to different results. In addition, a small number of time series in the Skagerrak region was used for tidal analysis, because not many trajectories reached the required minimum trajectory length. Thus, no exact values but trends for the tidal values in the Skagerrak can be provided. However, the analysis method confirms results by Otto et al. (1990), Ricker and Stanev (2020) or Meyerjürgens et al. (2019) that tidal currents are more pronounced in the shallow southern area of the North Sea (Fig. 6). The magnitudes for the maximum velocities during spring tides can also be confirmed, of up to 1 m s^{-1} in the shallow southern area of the North Sea, up to 0.1 m s^{-1} in the deeper northern area (Dietrich, 1950; Otto et al., 1990), and magnitudes of 1 cm s^{-1} in the Skagerrak (Danielssen, 1997; Rodhe, 1987). In addition, the orientation of the southern tidal ellipses shows the distinct east-west motion in the shallow area of the North Sea, which changes to a north-south motion toward the deeper North Sea, consistent with the description of Otto et al. (1990).

6 Summary and Conclusion

The results of the Lagrangian dataset provide valuable insights into current and tidal dynamics in the North Sea region. The calculated values are in agreement with models and in-situ measurements, and provide an area covering measurement method in contrast to Euler methods and a higher resolution in contrast to remote sensing and satellite methods. A number of computational methods have been presented that can provide a gridded overview of mean residual circulations and tidal dynamics in the North Sea, which can also be used for other areas. It is important to note that accurate tidal and current analysis can only be generated if measurements are made over long time periods shown in this study for the North Sea. The results show clear distinguish current patterns between the deep part in the Skagerrak and the southern shallow area of the North Sea. The southern shallow water shelf area shows little residual circulation, but is strongly influenced by the dynamics of the tides. In contrast, the deep area of the North Sea shows only minor contribution by the tides to the circulation, but strong transport processes by the residual circulations are dominant, which are influenced by high density gradients.

In the future, these measurements can be complemented by further drifter deployments to provide even higher resolution for current and tidal analysis for accurate values, to detect long-term variations, and to cover a larger spatial domain.

https://doi.org/10.5194/essd-2023-359
Preprint. Discussion started: 24 October 2023

In addition, sensory developments of the drifter are beneficial. For example, the sampling rate can be adapted to the deployment strategy, depending on the drifter deployment duration or whether mesoscale or submesoscale processes are analyzed. Furthermore, due to the fine sampling rate and by using additional measurement parameters, such as temperature and salinity, the sensory developments could support for example the analyses of ocean front and slick dynamics, as well as weather forecast models.

The dataset should be used for further analysis to provide additional insights for various marine research topics. Global marine litter transport models that previously excluded the North Sea due to the lack of data (Van Sebille et al., 2012; Maximenko et al., 2012) can be extended and areas of particle accumulation can be located. The dataset can be used to determine eddy kinetic energy and other submesoscale processes, and likewise analysis methods from well-studied regions, such as the Gulf Stream region (Lilly and Pérez-Brunius, 2021b; Oscroft et al., 2020), can be applied to the North Sea region.

Data Availability

The drifter dataset is available at https://cloud.uol.de/s/nyF4SfTTMYbSkk9. It is in the publication process at the Pangaea database, the DOI link will be available in 4-6 weeks and subsequently provided in this manuscript. The dataset contains the interpolated drifter position data, the drifter derived current velocities and two vectors (“beached” and “filled”) describing when a drifter was beached and when the dataset was filled because no GPS position was sent for more than one hour.

Funding

This study was carried out within the projects "Macroplastics Pollution in the Southern North Sea-Sources, Pathways and Abatement Strategies" (grant no. ZN3176) and “Sailing Intelligent Micro Drifter Swarms” (grant no. ZN3685) funded by the German Federal State of Lower Saxony, "Carbon Storage in German Coastal Seas - Stability, Vulnerability and Perspectives for Manageability" (grant no. 03F0875C) funded by Federal Ministry of Education and Research and "Biogeochemical processes and Air-sea exchange in the Sea-Surface microlayer" (grant no. 451574234) funded by German Research Foundation.

Author Contribution

LD performed to the data analysis. LD and JM prepared the draft of the manuscript. JM and THB proposed the scientific idea of the manuscript and performed the data acquisition. All authors contributed to the critical revision of the article and provided important advice for the improvement of the manuscript.

https://doi.org/10.5194/essd-2023-359
Preprint. Discussion started: 24 October 2023

Conflict of Interest

The authors declare that they have no conflict of interest.

Acknowledgments

We would like to thank the master and crew onboard the RV Heincke HE503, HE520, HE527, HE583, HE586, and Alkor AL523 for supporting the deployments of the drifters. This allowed the collection of large datasets. We thank Axel Braun, Andreas Sommer, Elisa Janssen, Michael Butter and Lars Meyer-Hagg for the support in constructing the drifters.

References

Baschek, B., Schroeder, F., Brix, H., Riethmüller, R., Badewien, T. H., Breitbach, G., Brügge, B., Colijn, F., Doerffer, R., Eschenbach, C., Friedrich, J., Fischer, P., Garthe, S., Horstmann, J., Krasemann, H., Metfies, K., Merckelbach, L., Ohle, N., Petersen, W., Pröfrock, D., Röttgers, R., Schlüter, M., Schulz, J., Schulz-Stellenfleth, J., Stanev, E., Staneva, J., Winter, C., Wirtz, K., Wollschläger, J., Zielinski, O., and Ziemer, F.: The Coastal Observing System for Northern and Arctic Seas (COSYNA), Ocean Sci., 13, 379–410, https://doi.org/10.5194/os-13-379-2017, 2017.

Becker, G. A., Giese, H., Isert, K., König, P., Langenberg, H., Pohlmann, Th., and Schrum, C.: Mesoscale structures, fluxes and water mass variability in the German Bight as exemplified in the KUSTOS- experiments and numerical models, Dtsch. Hydrogr. Z., 51, 155–179, https://doi.org/10.1007/BF02764173, 1999.

Burchard, H. and Badewien, T. H.: Thermohaline residual circulation of the Wadden Sea, Ocean Dyn., 65, 1717–1730, https://doi.org/10.1007/s10236-015-0895-x, 2015.

Danielssen, D.: Oceanographic variability in the Skagerrak and Northern Kattegat, May–June, 1990, ICES J. Mar. Sci., 54, 753–773, https://doi.org/10.1006/jmsc.1996.0210, 1997.

Davies, A. M. and Furnes: Observed and Computed M_2 Tidal Currents in the North Sea, J. Phys. Oceanogr., 10, 237–257, https://doi.org/10.1175/1520-0485(1980)010<0237:OACMTC>2.0.CO;2, 1980.

Dempster, J.: The Laboratory Computer: A Practical Guide for Physiologists and Neuroscientists, Academic Press, London, 136–171 pp., 2001.

Dietrich, G.: Die natürlichen Regionen von Nord- und Ostsee auf hydrographischer Grundlage, Kiel. Meeresforsch., 7, 35–69, 1950.

Essink, S., Hormann, V., Centurioni, L. R., and Mahadevan, A.: Characterizing ocean kinematics from surface drifters, Oceanography, https://doi.org/10.1002/essoar.10504137.1, 2020.

Fritsch, F. N. and Carlson, R. E.: Monotone Piecewise Cubic Interpolation, SIAM J. Numer. Anal., 17, 238–246, https://doi.org/10.1137/0717021, 1980.

Howarth, M. J.: NORTH SEA CIRCULATION, Enclopedia Ocean Sci. Second Ed., 73–81, 2001.

Huthnance, J.: Physical oceanography of the North Sea, Ocean Shorel. Manag., 16, 199–231, https://doi.org/10.1016/0951-8312(91)90005-M, 1991.

Le Provost, C.: Generation of overtides and compound tides (review), in: Tidal Hydrodynamics, John Wiley and Sons Inc, New York, 269–296, 1991.

Lilly, J. M. and Pérez-Brunius, P.: A gridded surface current product for the Gulf of Mexico from consolidated drifter measurements, Earth Syst. Sci. Data, 13, 645–669, https://doi.org/10.5194/essd-13-645-2021, 2021a.

Lilly, J. M. and Pérez-Brunius, P.: Extracting statistically significant eddy signals from large Lagrangian datasets using wavelet ridge analysis, with application to the Gulf of Mexico, Nonlinear Process. Geophys., 28, 181–212, https://doi.org/10.5194/npg-28-181-2021, 2021b.

Liu, Y. and Weisberg, R. H.: Evaluation of trajectory modeling in different dynamic regions using normalized cumulative Lagrangian separation, J. Geophys. Res., 116, C09013, https://doi.org/10.1029/2010JC006837, 2011.

Lumpkin, R., Özgökmen, T., and Centurioni, L.: Advances in the Application of Surface Drifters, Annu. Rev. Mar. Sci., 9, 59–81, https://doi.org/10.1146/annurev-marine-010816-060641, 2017.

Maas, L. R. M. and van Haren, J. J. M.: Observations on the vertical structure of tidal and inertial currents in the central North Sea, J. Mar. Res., 45, 293–318, https://doi.org/10.1357/002224087788401106, 1987.

Martín, J., Alonso, G., Dragani, W., Meyerjürgens, J., Giesecke, R., Cucco, A., and Fenco, H.: General circulation and tidal wave propagation along the Beagle Channel, J. Mar. Syst., 240, 103889, https://doi.org/10.1016/j.jmarsys.2023.103889, 2023.

Maximenko, N., Hafner, J., and Niiler, P.: Pathways of marine debris derived from trajectories of Lagrangian drifters, Mar. Pollut. Bull., 65, 51–62, https://doi.org/10.1016/j.marpolbul.2011.04.016, 2012.

McWilliams, J. C.: Submesoscale currents in the ocean, Proc. R. Soc. Math. Phys. Eng. Sci., 472, 20160117, https://doi.org/10.1098/rspa.2016.0117, 2016.

McWilliams, J. C.: A survey of submesoscale currents, Geosci. Lett., 6, 3, https://doi.org/10.1186/s40562-019-0133-3, 2019.

Meyerjürgens, J., Badewien, T. H., Garaba, S. P., Wolff, J.-O., and Zielinski, O.: A State-of-the-Art Compact Surface Drifter Reveals Pathways of Floating Marine Litter in the German Bight, Front. Mar. Sci., 6, https://doi.org/10.3389/fmars.2019.00058, 2019.

Meyerjürgens, J., Ricker, M., Schakau, V., Badewien, T. H., and Stanev, E. V.: Relative Dispersion of Surface Drifters in the North Sea: The Effect of Tides on Mesoscale Diffusivity, J. Geophys. Res. Oceans, 125, https://doi.org/10.1029/2019JC015925, 2020.

Meyerjürgens, J., Ricker, M., Aden, C., Albinus, M., Barrelet, J., Freund, H., Hahner, F., Lettmann, K. A., Mose, I., Schaal, P., Schöneich-Argent, R. I., Stanev, E. V., Wolff, J.-O., Zielinski, O., and Badewien, T. H.: Sources, pathways, and abatement strategies of macroplastic pollution: an interdisciplinary approach for the southern North Sea, Front. Mar. Sci., 10, 1148714, https://doi.org/10.3389/fmars.2023.1148714, 2023.

Oscroft, S., Sykulski, A. M., and Early, J. J.: Separating Mesoscale and Submesoscale Flows from Clustered Drifter Trajectories, Fluids, 6, 14, https://doi.org/10.3390/fluids6010014, 2020.

https://doi.org/10.5194/essd-2023-359
Preprint. Discussion started: 24 October 2023

Otto, L., Zimmerman, J. T. E., Furnes, G. K., Mork, M., Saetre, R., and Becker, G.: REVIEW OF THE PHYSICAL OCEANOGRAPHY OF THE NORTH SEA, Neth. J. Sea Res., 26, 161–238, https://doi.org/10.1016/0077-7579(90)90091-T, 1990.

Özgökmen, T. M., Poje, A. C., Fischer, P. F., Childs, H., Krishnan, H., Garth, C., Haza, A. C., and Ryan, E.: On multi-scale dispersion under the influence of surface mixed layer instabilities and deep flows, Ocean Model., 56, 16–30, https://doi.org/10.1016/j.ocemod.2012.07.004, 2012.

Pawlowicz, R., Beardsley, B., and Lentz, S.: Classical tidal harmonic analysis including error estimates in MATLAB using T_TIDE, Comput. Geosci., 28, 929–937, https://doi.org/10.1016/S0098-3004(02)00013-4, 2002.

Ricker, M. and Stanev, E. V.: Circulation of the European northwest shelf: a Lagrangian perspective, Ocean Sci., 16, 637–655, https://doi.org/10.5194/os-16-637-2020, 2020.

Ricker, M., Stanev, E., Badewien, T. H., Freund, H., Meyerjürgens, J., Wolff, J., and Zielinski, O.: Drifter observations and Lagrangian tracking of the 2018 easterly wind event in the North Sea, J. Oper. Oceanogr. - Copernic. Mar. Serv. Ocean State Rep., 13, S155–S160, 2020.

Ricker, M., Meyerjürgens, J., Badewien, T. H., and Stanev, E. V.: Lagrangian Methods for Visualizing and Assessing Frontal Dynamics of Floating Marine Litter with a Focus on Tidal Basins, in: The Handbook of Environmental Chemistry, Springer, Berlin, Heidelberg, 1–36, https://doi.org/10.1007/698_2021_812, 2021.

Rodhe, J.: The large-scale circulation in the Skagerrak; interpretation of some observations, Tellus A, 39A, 245–253, https://doi.org/10.1111/j.1600-0870.1987.tb00305.x, 1987.

Rodhe, J.: ON THE DYNAMICS OF THE LARGE-SCALE CIRCULATION OF THE SKAGERRAK, J. Sea Res., 35, 9–21, 1996.

Stanev, E. V. and Ricker, M.: Interactions between barotropic tides and mesoscale processes in deep ocean and shelf regions, Ocean Dyn., 70, 713–728, https://doi.org/10.1007/s10236-020-01348-6, 2020.

Stanev, E. V., Schulz-Stellenfleth, J., Staneva, J., Grayek, S., Grashorn, S., Behrens, A., Koch, W., and Pein, J.: Ocean forecasting for the German Bight: from regional to coastal scales, Ocean Sci., 12, 1105–1136, https://doi.org/10.5194/os-12-1105-2016, 2016.

Stanev, E. V., Badewien, T. H., Freund, H., Grayek, S., Hahner, F., Meyerjürgens, J., Ricker, M., Schöneich-Argent, R. I., Wolff, J.-O., and Zielinski, O.: Extreme westward surface drift in the North Sea: Public reports of stranded drifters and Lagrangian tracking, Cont. Shelf Res., 177, 24–32, https://doi.org/10.1016/j.csr.2019.03.003, 2019.

Sündermann, J. and Pohlmann, T.: A brief analysis of North Sea physics, Oceanologia, 53, 663–689, https://doi.org/10.5697/oc.53-3.663, 2011.

Tarry, D. R., Ruiz, S., Johnston, T. M. S., Poulain, P., Özgökmen, T., Centurioni, L. R., Berta, M., Esposito, G., Farrar, J. T., Mahadevan, A., and Pascual, A.: Drifter Observations Reveal Intense Vertical Velocity in a Surface Ocean Front, Geophys. Res. Lett., 49, https://doi.org/10.1029/2022GL098969, 2022.

Taylor, J. R. and Thompson, A. F.: Submesoscale Dynamics in the Upper Ocean, Annu. Rev. Fluid Mech., 55, 103–127,

https://doi.org/10.1146/annurev-fluid-031422-095147, 2023.

Valle-Levinson, A., Stanev, E., and Badewien, T. H.: Tidal and subtidal exchange flows at an inlet of the Wadden Sea, Estuar. Coast. Shelf Sci., 202, 270–279, https://doi.org/10.1016/j.ecss.2018.01.013, 2018.

Van Sebille, E., England, M. H., and Froyland, G.: Origin, dynamics and evolution of ocean garbage patches from observed surface drifters, Environ. Res. Lett., 7, 044040, https://doi.org/10.1088/1748-9326/7/4/044040, 2012.

Van Sebille, E., Aliani, S., Law, K. L., Maximenko, N., Alsina, J. M., Bagaev, A., Bergmann, M., Chapron, B., Chubarenko, I., Cózar, A., and others: The physical oceanography of the transport of floating marine debris, Environ. Res. Lett., 15, 023003, 2020.

Vindenes, H., Orvik, K. A., Søiland, H., and Wehde, H.: Analysis of tidal currents in the North Sea from shipboard acoustic Doppler current profiler data, Cont. Shelf Res., 162, 1–12, https://doi.org/10.1016/j.csr.2018.04.001, 2018.